Received: 24 February 2020 | Revised: 6 October 2020 | Accepted: 9 April 2021

DOI: 10.1002/pc.26078

RESEARCH ARTICLE

spe INSPIRING PLASTICS PROFESSIONALS Polymer COMPOSITES WILEY

A source-sink model for water diffusion in an activated carbon fiber/phenolic composite

Sue Alston[1] | **Cris Arnold**[1] | **Martin Swan**[2] | **Corinne Stone**[2]

[1]College of Engineering, Swansea University, Fabian Way, Swansea, UK

[2]Defence Science and Technology Laboratory, Porton Down, Salisbury, Wiltshire, UK

Correspondence
Cris Arnold, College of Engineering, Swansea University, Fabian Way, Swansea SA1 8EN, UK.
Email: j.c.arnold@swansea.ac.uk

Funding information
Defence Science and Technology Laboratory

Abstract

The moisture absorption behavior of a composite comprising phenolic resin and activated carbon fibers was characterized. The resin starts with a water content from curing and the active fibers both adsorb water on their surface and absorb water in sub-surface pores, acting as a sink or source of water. Measured data showed that the dependence of this water uptake on the surrounding relative humidity was highly nonlinear, and that the effective diffusion rate through the composite was very dependent on the starting and end conditions. A physically based model has been successfully developed to simulate this behavior. Diffusion was assumed to be Fickian and entirely through the resin, with a linear dependence of resin water content on external humidity. Water movement between resin and fibers was determined so as to maintain equilibrium, based on measured steady-state water uptake curves across a range of relative humidities. This meant that in mid-range humidities, most water movement was between fibers and resin rather than through the resin, giving low effective diffusion rates. This model and a simple Arrhenius expression for the diffusion coefficient through the resin enabled measured composite diffusion behavior to be accurately predicted over a range of temperatures and humidity changes.

KEYWORDS

adsorption, composites, computer modeling, diffusion

1 | INTRODUCTION

The mechanical properties of carbon fibers combined with the fire resistance or high-temperature capability of phenolic resins mean that carbon fiber/phenolic composites are used in a variety of demanding applications. These include systems where the material may experience extreme temperatures and rapid temperature changes, leading to mechanical and thermomechanical damage, such as in thermal protection systems for space or rocket applications.[1] In many cases, these materials may also have long-term exposure to water from humid air or direct water contact, and so studying such behavior is important. There are some features of such materials that make the interaction with water somewhat different from other composites, warranting different approaches.

The polymerization of phenolic resins is through a condensation reaction which results in a small amount of water remaining in the material when curing is complete. This may be a few percent by weight and may change

during subsequent storage. Since this may affect the resin properties, the ability to predict water diffusion behavior through the composite after manufacture is of importance. There may also be variation in the carbon fibers used, which may be fully graphitized and assumed to hold no water. However, in some cases, activated carbon fibers that retain some porosity can be used, and these were of particular interest in this work. These are able to adsorb water on the surface and to absorb water in the subsurface pores, although it is assumed that this does not lead to diffusion through the fibers. Previous work by Stokes[2] had suggested that the dependence of the water uptake of such fibers on humidity was significantly nonlinear and this had potential implications for the diffusion behavior.

Modeling of water diffusion through polymer resins is generally based on Fick's equations during the early stages, while during long-term conditioning, many resins then show a gradual slow water uptake after the initial Fickian behavior.[3] For carbon fiber composite material, it is typically assumed that diffusion takes place entirely through the resin, with no water present in the fibers. The diffusion rate through the composite is determined by its microstructure, since the fibers can act as barriers leading to longer diffusion pathways. For a typical laminate structure, diffusion along the fiber direction is generally similar to that through the resin alone, while diffusion across and through the plies is considerably slower.[4]

For fibers that absorb water, for example, natural fibers, there may also be diffusion through the fibers, but this is generally also assumed to be Fickian with the fibers and resin in equilibrium. A similar case applies for a woven structure where individual tows of fibers closely surrounded by resin can be modeled as a separate material with a different diffusion coefficient from larger regions of neat resin between tows.[5] However, porous carbon fibers are unlike these, since there is no Fickian or similar diffusion through them; rather water will be adsorbed on to or absorbed into the fibers, which can act as a sink or source of water to the resin, so affecting the diffusion process.

The complexity of this type of system means that a number of issues need to be considered. This includes whether the diffusion through the resin is Fickian, and the dependence of the water content of the resin and fibers on the surrounding relative humidity, as well as how to deal with the nondiffusive nature of the fiber water content.

Fick's laws alone assume no interaction between the water and the material through which it is diffusing, but there are several approaches to modifying this for cases where there is interaction. Carter and Kibler[6] developed a Langmuir-type hindered diffusion model which distinguished mobile molecules moving through the medium from bound and therefore stationary molecules. Probabilities β and γ were defined for the rate at which molecules moved between the two states. The reasons for molecules becoming bound did not need to be specified but could include voids, hydrogen bonding, heterogeneous morphology, or Van der Waals interactions.[7] Grace and Altan[8] successfully applied this model to various resins and glass and carbon fiber composites, while Popineau et al.[9] obtained a good fit for an epoxy adhesive. In these cases, the interactions were between the diffusing molecules and the polymer resin. Liu et al.[10] compared three models, including a Langmuir-type model, applied to water diffusion through a vinyl ester/clay nano-composite. In this case, diffusion was hindered by adsorption of water molecules on the clay particles as well as any interaction with the polymer. In the above cases, the model was fitted to measured data for individual water uptake curves using a number of parameters including diffusion coefficient and the probabilities of molecules moving between bound and unbound states. Popineau et al.[9] and Rodriguez et al.[7] were able to derive Arrhenius relationships between these parameters and temperature.

The model development described here ran alongside an extensive experimental program, which provided data to guide the modeling on a continual basis. This suggested that the movement of water between fibers and resin was strongly and nonlinearly dependent on water content so unlikely to be represented by fixed values of β and γ. An alternative approach was therefore developed using the "source-sink" concept referred to above and was intended to simulate shorter-term water uptake or loss rather than any longer-term behavior.

Two components came together to give the overall model. First, data were available giving the dependence of water content in the resin, composite, and fibers on relative humidity and temperature. Although this was very nonlinear, it could be represented by equations based on known physical processes. These equations determined the equilibrium between resin and fibers, and hence the amount of water moving between the two as a function of water content and temperature. The majority of parameters required for the overall model were therefore derived from steady-state water content data. Second, diffusion through the resin was assumed to be Fickian over the timescale being considered, with a temperature-dependent diffusion coefficient. The Arrhenius parameters of this were the only ones which needed to be obtained from dynamic uptake data.

As well as the factors already mentioned, diffusion of water through a composite material can depend on the

fiber surface treatment and its effect on the interphase region.[11] This effect is not explicitly modeled in this work, although it will have influenced the model parameters obtained. This is discussed in the appropriate sections below.

This model was developed from data related to a carbon fiber/phenolic composite where the fibers had some porosity, in order to predict water content during use. However, it could also be of use in other applications. Porous carbon fibers can be used to increase the protection from electromagnetic radiation[12,13] to absorb volatile organic compounds[14,15] or to act as a scaffold for tissue regeneration.[16] The presence of water may affect performance and the ability to predict water content would therefore be of benefit. Other applications may be where a resin is in contact with an alternative non-absorbing medium with some porosity, such as nano-fillers, or substrates with pinhole defects. Some more diverse applications could be in predicting the diffusion of water causing degradation in polymer solar cells[17] or in biopolymers in implantable biomedical devices,[18] or the time taken for a solvolysis process to break down thermoset composites for recycling.[19]

2 | MATERIALS

The carbon fiber/phenolic composite material used a commercially available resole phenolic resin, reinforced with a woven carbon fabric using activated carbon fibers that retain some porosity. Composite panels were clave-cured in a commercial manufacturing process. Exact material details and treatment were commercially confidential; however, the possible effects of these are discussed in the relevant sections below. Thin disk samples approximately 25 mm in diameter and 1 mm in thickness were machined from thicker panels. All samples tested were from the same batch of original manufacture.

3 | EXPERIMENTAL

Water absorption/desorption experiments were carried out on samples moved between a range of different humidities as detailed in Table 1. Conditions were generated from one of (a) controlled climate chamber (b) desiccant in a jar in an oven or (c) above saturated salt solution in a jar in an oven using a suitable salt. The nominal humidities used were dry, 25%RH, 45%RH, 65% RH, and 85%RH. Salts were selected to give humidities as close as possible to these, but the actual values were slightly different, as specified in Table 1.

Samples were weighed using a high-precision analytical balance at intervals approximating to 1 √hour throughout conditioning.

The as-manufactured water content was deduced from as-received samples that were dried and lost approximately 4% of their weight. This then meant that those conditioned at 85%RH had an overall water content of about 9.5%. Figure 1 shows the water uptake and loss for various of the condition changes at 70°C, plotted against √time/thickness to remove any effects of sample thickness differences. It can be seen that the time taken to reach a steady state varied considerably according to the start and end conditions. For example, samples dried from the as-manufactured condition reached their dry state in less than 20 √hours/mm, while those conditioned from dry to 65%RH took closer to 40 √hours/mm.

Tests carried out on the same resin alone (i.e., without fibers) had shown that the steady-state

TABLE 1 Sample conditioning matrix

Temperature (°C)	Starting RH (%)	Conditioning RH levels (%)				
23	Dry					85
	As-manufactured	0	23		68	85
	85	0				
40	As-manufactured	0	22	43	63	80
	85	0				
50	Dry					85
	As-manufactured	0	30		68	85
	85	0				
70	Dry		28	45	65	85
	45	0				85
	As-manufactured	0	28		65	85
	85	0		45		

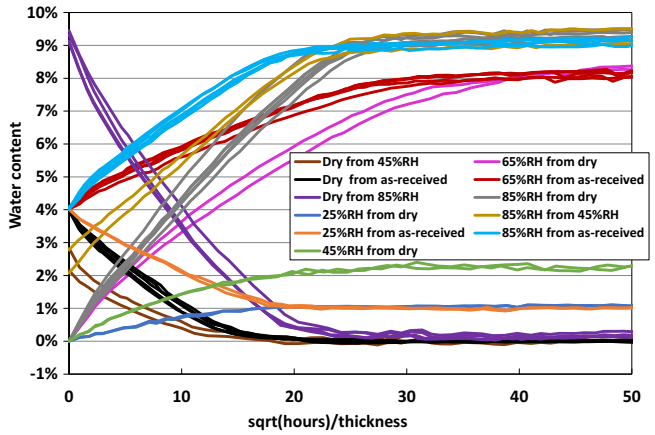

FIGURE 1 Water content graphs for samples conditioned at 70°C [Color figure can be viewed at wileyonlinelibrary.com]

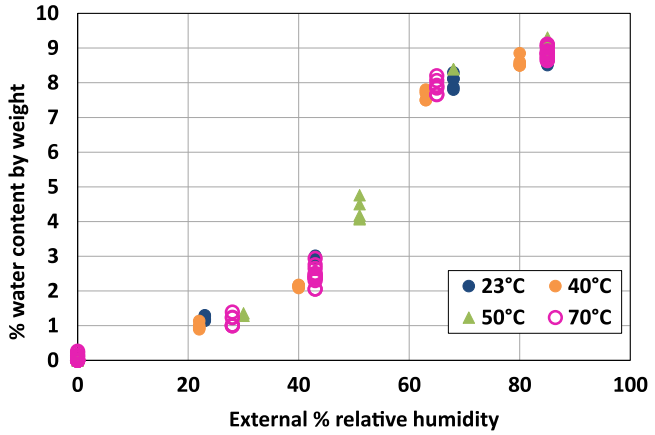

FIGURE 2 Steady-state water content of composite samples at various external humidity values [Color figure can be viewed at wileyonlinelibrary.com]

water content varied linearly with relative humidity (RH) and reached 6% at 100%RH. The composite conditioning produced the steady-state water content curve as shown in Figure 2, which was clearly not linear. There appeared to be little effect of temperature, although further investigation as described below identified some differences particularly at lower humidities.

Conditioning tests on the carbon fabric alone were also carried out. The rate of water loss or gain for the fibers was very fast so the weight had to be measured *in situ*, using a dynamic vapor sorption unit. The results are shown in Figure 3 and had a similar sigmoidal shape.

This behavior of a porous carbon fiber and corresponding composite agreed with that from Stokes.[2] It was attributed to the presence of at least two water-absorbing phases. Investigation of the mechanism for water ingress to and egress from these fibers by Do and

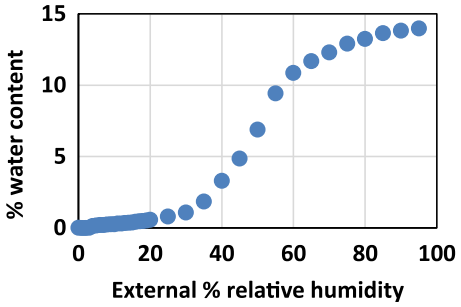

FIGURE 3 Steady-state water content of carbon fabric samples as a function of external humidity [Color figure can be viewed at wileyonlinelibrary.com]

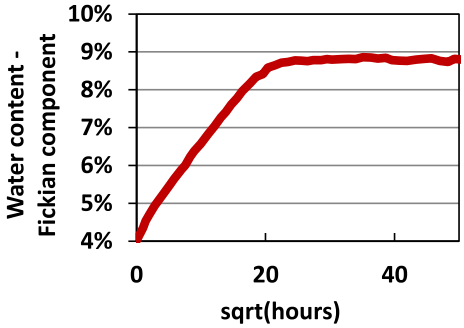

FIGURE 4 Example of Fickian component of weight change curve (70°C, as-received to 85%RH) [Color figure can be viewed at wileyonlinelibrary.com]

Do[15] proposed that water was initially adsorbed on to the fiber surface, then migrated into the pores when sufficiently large clusters of water molecules had built up.

The individual weight change curves were mainly linear up to around 75% of the total change, apart from a steeper section at the very start which was attributed to exposed fibers from machining. Longer-term conditioning showed a gradual weight increase; however, the aim of this exercise was to simulate the Fickian part of the behavior while taking account of the different rate of change at different humidities. The longer-term behavior was therefore removed so as to extract the Fickian part of the change from each curve. An example is shown in Figure 4.

An "effective" diffusion coefficient was calculated from the curve for each sample. The overall diffusion rate would have been driven by a combination of the rates through the sample thickness and from the edges, which would have been at different rates as a result of the detailed microstructure. The complexity of the woven structure meant that these separate rates could not be identified and so a single average value was assumed. However, the sample dimensions meant that in any case

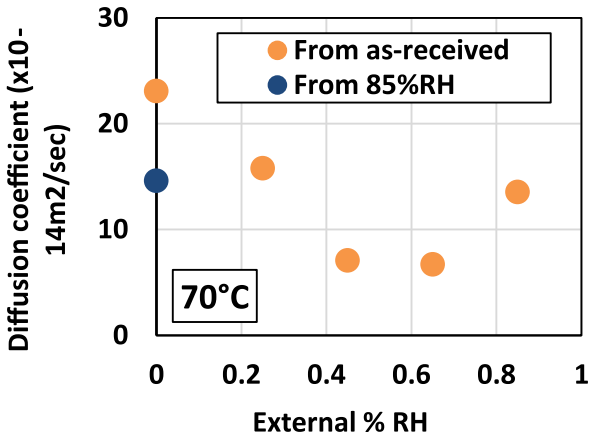

FIGURE 5 Effective diffusion coefficients for samples conditioned at 70°C [Color figure can be viewed at wileyonlinelibrary.com]

diffusion through the thickness dominated, and it was found that a one-dimensional (1D) approximation gave sufficiently close results to a full three-dimensional fit. The 1D analytical form (Equation 1) for the linear part of Fickian diffusion could therefore be used.

$$\frac{M_t}{M_\infty} = \frac{4}{h}\sqrt{\frac{tD}{\pi}} \tag{1}$$

where M_t is the weight change at time t, M_∞ is the total weight change when a steady state is reached, t is the conditioning time, h is the sample thickness, and D is the effective diffusion coefficient.

Across all the samples, the most linear part of the curve was found to be between 30% and 70% of the total change. Equation (1) can be rewritten to give D as in the following equation:

$$D = \left(\frac{\pi h^2}{16}\right)\left(\frac{\text{Gradient}}{M_\infty}\right)^2 \tag{2}$$

where Gradient is the gradient of the weight change versus √secs graph over the selected range, and this was used to obtain the effective diffusion coefficient for each sample.

Confirming the visual evidence from Figure 1, the effective diffusion coefficients were found to depend strongly on humidity. For example, the values for samples conditioned at 70°C from the as-manufactured state are shown in Figure 5. Also included (in blue) is the effective diffusion coefficient for samples going from 85% RH to dry, showing that both the starting and final humidity affect the behavior.

4 | MODEL DERIVATION

The data obtained showed clearly that the effective diffusion coefficient of the composite depended on the starting and finishing water content. It also indicated that the fibers were acting as a source or sink of water, with the amount very dependent on relative humidity. The aim was first to develop a model which predicted the water content in resin and fibers as a function of relative humidity, without assuming linearity in either case. This would be combined with a Fickian diffusion process through the resin, to find out whether this simulated the observed effective diffusion through the composite. It was assumed that there was no energy barrier to water movement between resin and fibers. The derivation followed that for Fickian diffusion but with expanded equations for concentration and diffusion coefficient.

Fick's second law in three dimensions can be written as

$$\frac{\partial c}{\partial t} = D\underline{\nabla}.(\underline{\nabla} c) \tag{3}$$

where c is the concentration of water in the material and D is the diffusion coefficient. This formulation is useful for a single material, however at a material boundary, such as between resin and fibers, the concentration is not necessarily continuous, and it is convenient to use an alternative parameter. In this work, the moisture distribution in a sample is characterized by the parameter a, referred to as "activity." This is dimensionless and continuous across material boundaries. At the sample surface, it is equal to the external relative humidity. In a resin system where the moisture concentration is linearly dependent on RH, it corresponds to the value often called "relative concentration" = "concentration/concentration at 100% RH." It is closely related to thermodynamic "activity" hence the terminology.

In this case, a number of the variables contributing to this equation were potentially nonlinearly dependent on activity. The data in Figures 2 and 3 make it clear that this was true for the water content of the fibers. Although it appeared that the resin water content was linearly dependent on activity, the extended version of the diffusion equations has been derived without making this assumption. The behavior of the resin diffusion coefficient was unclear at this stage so again no assumptions were made.

The model equations are derived from the continuity equation

$$\frac{\partial c}{\partial t} + \underline{\nabla}.\underline{J} = 0 \tag{4}$$

where c is the mass concentration (kg/m^3) and $\underline{J}$ is the mass flux (kg/[m^2.s]).

The overall concentration c is a combination of water content in the resin and that in the fibers, that is,

$$c(a) = (1 - V_f)c_R(a) + V_f c_F(a) \tag{5}$$

where a is the activity (dimensionless), V_f is the fiber volume fraction (dimensionless), c_R is the water concentration in resin (kg/m^3), and c_F is the water concentration in fibers (kg/m^3).

Across any area, the flux $\underline{J}$ is the average over resin and fibers. Using Fick's first law, and assuming the diffusion coefficient for fibers to be zero, this gives

$$\underline{J} = -(1 - V_f)D_R(a)\underline{\nabla}c_R(a) = -(1 - V_f)D_R(a)\frac{dc_R}{da}\underline{\nabla}a \tag{6}$$

where D_R is the average diffusion coefficient through the resin in the composite (m^2/s). In general, this can be calculated as

$$D_R = kD_{\text{Resin}} \tag{7}$$

where D_{Resin} is the diffusion coefficient through the resin and k is a factor representing the microstructure. Since all samples in this case were manufactured from the same material in the same way, k should have varied little between samples, and this was confirmed by the measured data.

From Equations (4), (5), and (6),

$$\left[(1 - V_f)\frac{dc_R}{da} + V_f\frac{dc_F}{da}\right]\frac{\partial a}{\partial t} + \underline{\nabla}.\left(-(1 - V_f)D_R\frac{dc_R}{da}\underline{\nabla}a\right) = 0 \tag{8}$$

which can be re-written as

$$\propto (a)\frac{\partial a}{\partial t} = \underline{\nabla}.(\beta(a)\underline{\nabla}a) \tag{9}$$

$$\propto = \frac{dc_R}{da} + \frac{V_f}{(1 - V_f)}\frac{dc_F}{da} \tag{10}$$

$$\beta = D_R(a)\frac{dc_R}{da} \tag{11}$$

Under certain conditions, this can be simplified. For example, for a case such as epoxy resin with fully graphitized carbon fibers, c_R is linearly dependent on a, the fibers contain no water so $c_F = 0$, and the diffusion coefficient is independent of activity. Equation (9) then reduces to the standard version of Fick's second law.

The effective diffusion behavior now depends not only on the diffusion coefficient D_R but also on whether water is moving in/out of the fibers or progressing through the resin. A useful indicator of this is the resin transport ratio, that is, the fraction F of water movement, which is through the resin rather than migration into or out of the fibers. If F is high, that is, water moves through the resin, then overall diffusion is faster. If F is low, then more of the water is moving between resin and fibers and not progressing through the resin, so overall diffusion is lower. This can be expressed as $F = dw_R/(dw_R + dw_F)$, where dw_R is the change in the mass of water in the resin and dw_F is the change in the mass of water in the fibers, over a time step Δt in a cell of unit volume. After further manipulation, this gives

$$F = \frac{\frac{dc_R}{da}}{\propto} \tag{12}$$

5 | MODELS FOR WATER CONTENT AND DIFFUSION COEFFICIENT

As already discussed, the water content of the resin alone had been found to be linearly dependent on activity, that is,

$$c_R(a) = s_R a \tag{13}$$

where s_R is the resin saturation water content (kg/m^3), that is, value at 100% activity.

If the diffusion coefficient through the resin had any dependence on water content, it would be expected to increase as water content increased as a result of plasticization. However, any attempt to use this approach to simulate the composite behavior failed, and it appeared that a fixed value of D_R regardless of activity was more appropriate. The diffusion coefficient could however be assumed to change with temperature, and a standard Arrhenius relationship was used as in the following equation:

$$D_R = D_0\exp\left(-\frac{E_a}{RT}\right) \tag{14}$$

where D_0 is the temperature-independent pre-exponential (m^2/s), E_a is the activation energy (J/mol), R

is the gas constant (J/mol-K), and T is the sample temperature (K).

The water content of the fibers was believed to comprise two parts; water molecules adsorbed on to the fiber and pore surface, and clusters of molecules absorbed into the pores.[15] At lower activity levels, adsorption dominated as individual molecules attached themselves to the surface, and this process appeared linear with activity. When sufficiently large clusters of molecules had formed, these migrated into the pores. Once started, this process followed a sigmoidal pattern through mid-level activities until it eventually leveled off as the pores became full. Equation (15) was used to describe this behavior,

$$c_F(a) = s_a\left(\min\left(\frac{a}{a_{\lim}},1\right)\right) + \frac{s_p}{(1+\exp(a_F))^{\nu}} \tag{15}$$

where s_a is the saturation for adsorbed water content (kg/m^3), that is, value at 100% activity. s_p is the saturation for pore water content (kg/m^3), that is, value at 100% activity, so that fiber water content at 100% activity, $s_F = s_a + s_p$. $a_{\lim}$ is the activity above which no more adsorption takes place (dimensionless)

$$a_F = \frac{\chi_F - a}{\sigma_F} \tag{16}$$

χ_F, σ_F, and ν are parameters determining the shape of the sigmoid (all dimensionless).

The two parameters s_a and s_p were found to be temperature dependent and calculated as

$$s_a = s_{a0}\exp\left(-\frac{E_{aa}}{\mathrm{RT}}\right) \text{and } s_p = s_{p0}\exp\left(-\frac{E_{ap}}{\mathrm{RT}}\right) \tag{17}$$

where T is the sample temperature (K).

Adsorption is generally an exothermic reaction, so following Le Chatelier's principle, it will decrease as temperature increases, and the dependency for s_a matched this. The pore absorption s_p increased with increasing temperature, corresponding to the air remaining in the pores having a greater capacity at absorb water at higher temperature.

The value of s_R was set based on previous resin measurements, and the parameters $a_{\lim}$, χ_F, σ_F, ν, s_{a0}, E_{aa}, s_{p0}, and E_{ap} were then tuned to best fit the measured composite concentration curve (the Solver function in Excel was used for this). The values used are detailed in Table 2.

Figure 6 shows the surface adsorption and pore absorption curves at the four main temperatures used for measurements, on separate y-axis scales. Figure 7 combines these and the resin water content to show the predicted composite water content curves, compared to measured data. The increased adsorption at lower temperature is clear in the curves up to 40% activity. At higher activity, when pore absorption becomes more significant, the curves become more similar and at maximum activity the overall concentration is slightly higher for higher temperature.

An example of the resin transfer ratio given by Equation (12), resulting from the parameters in Table 2 is shown in Figure 8. It can be seen that in the mid-activity range, the proportion of water being transported through the resin is small, at around 10%, while most is migrating in or out of the fibers.

6 | FINITE ELEMENT IMPLEMENTATION

The implementation was originally based on programs published by Smith and Griffiths,[20] who provided a time-stepping linear solver for the basic diffusion equation based on the Galerkin method with a preconditioned conjugate gradient optimization. This was modified to cater for the extended equations, but there was also the issue that Equation (9) is clearly nonlinear. Following the procedure used by Huo et al.,[21] this was dealt with by calculating α and β based on the activity a at the start of each time step then keeping them constant while updating a for that time step. This was valid so long as the time step was kept sufficiently short in relation to the sample being modeled. Since α and β are also temperature dependent, this re-calculation could also allow for simulation in a changing temperature environment.

The disk samples were meshed using three-dimensional brick elements with finer resolution at the exposed surfaces, as shown in Figure 9. The disk center was dealt with by creating wedge-shaped "brick" elements as illustrated in the lower diagram (shown in 2D). In each vertical layer, the central nodes were shared by

TABLE 2 Fitted parameters for modeling of fiber water content

Parameter	χ_F (%/100)	σ_F (%/100)	ν (dimensionless)	$a_{\lim}$ (%/100)
Value	0.53	0.047	1	0.53
Parameter	s_{a0} (kg/m^3)	E_{aa} (kJ/mol)	s_{p0} (kg/m^3)	E_{ap} (kJ/mol)
Value	0.19	−12.97	411.6	2.145

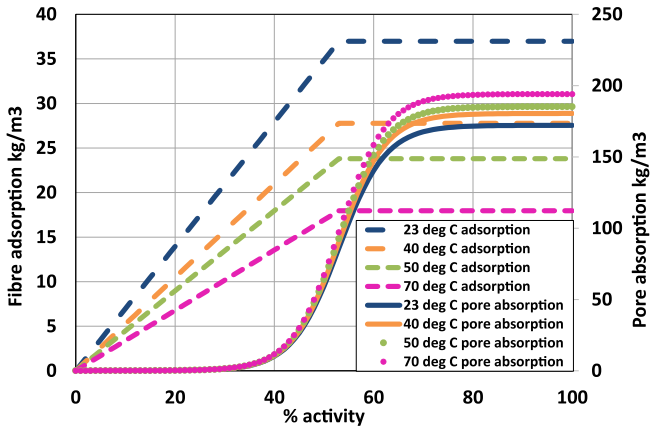

FIGURE 6 Modeled carbon fabric water content—fiber adsorption and pore absorption components [Color figure can be viewed at wileyonlinelibrary.com]

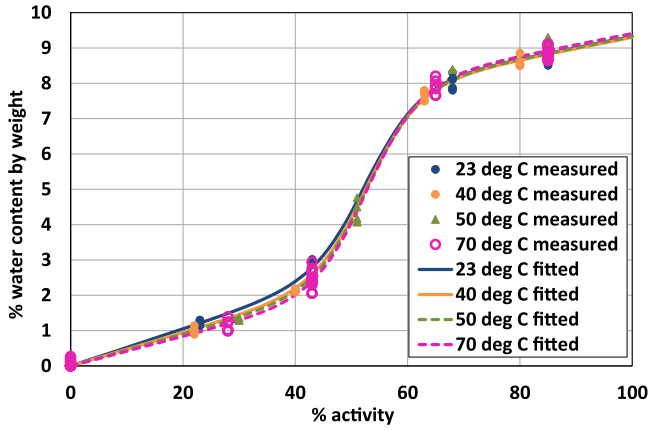

FIGURE 7 Modeled and measured composite water content data [Color figure can be viewed at wileyonlinelibrary.com]

all the wedge elements of that layer, giving a single connected network covering the whole sample. All surface nodes were set to an activity value corresponding to the external relative humidity. Sensitivity checks were carried out on both the mesh size and spacing, resulting in 23,400 elements. Despite the effect of the fibers, the time dependency of the measured behavior was still approximately linear with √time, so in order to reduce computation time this dependency was replicated, that is, the time step was expressed in √seconds. Sensitivity checks suggested that a value of 5 √seconds was appropriate.

7 | MODEL TUNING

With the concentration curves described above, only the diffusion coefficient through the resin remained unknown. Although some experimental data were available for samples made from the resin alone, there were

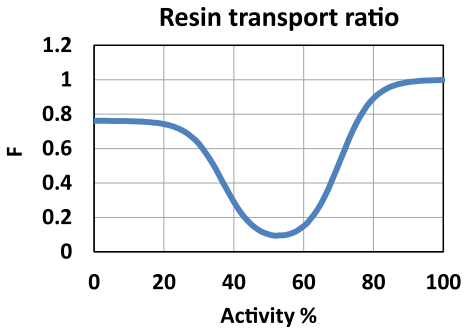

FIGURE 8 Resin transport ratio as a function of activity [Color figure can be viewed at wileyonlinelibrary.com]

reasons why these could not be used directly. The microstructure factor k (Equation 7) was unknown, although this could have been assumed to be the same across all temperatures and humidities. More significantly, it was believed that there were some important differences between the resin produced alone and the resin in the composite. This appeared to be partly due to differences in curing behavior and partly due to additional constraints when the fibers were present. As an example, the resin samples alone indicated a diffusion coefficient that varied with water content, but this did not fit the observed behavior of the resin in the composite. Consequently, the diffusion coefficient through the resin in the composite (D_R) was assumed to be unknown but independent of water content. It was therefore necessary to identify its value at each of the temperatures for which measured data were available and to convert this into an Arrhenius expression to predict the values at any temperature.

For each temperature, an initial estimate of D_R was made, then each humidity change was simulated for which data were available. An effective diffusion coefficient was then calculated from Equation (2) as for the measured data. Based on these results D_R for that temperature was adjusted manually to optimize the matches between measured and predicted effective diffusion coefficients. Since the model would normally be used to predict the behavior of real samples which would start from the as-manufactured state, the optimization was based on such samples. Tuning of D_R was an iterative process, resulting in a set of values for each of the temperatures 23, 40, 50, and 70°C. An Arrhenius plot of these results is shown in Figure 10(A).

This gave corresponding activation energy $E_a = 41.3$ kJ/mol and pre-exponential $D_0 = 8.31 \times 10^{-7}$ m^2/s. This can be compared with the measured "effective" activation energies for composite samples conditioned from the as-manufactured state, as shown in Figure 10(B). These were clearly dependent on

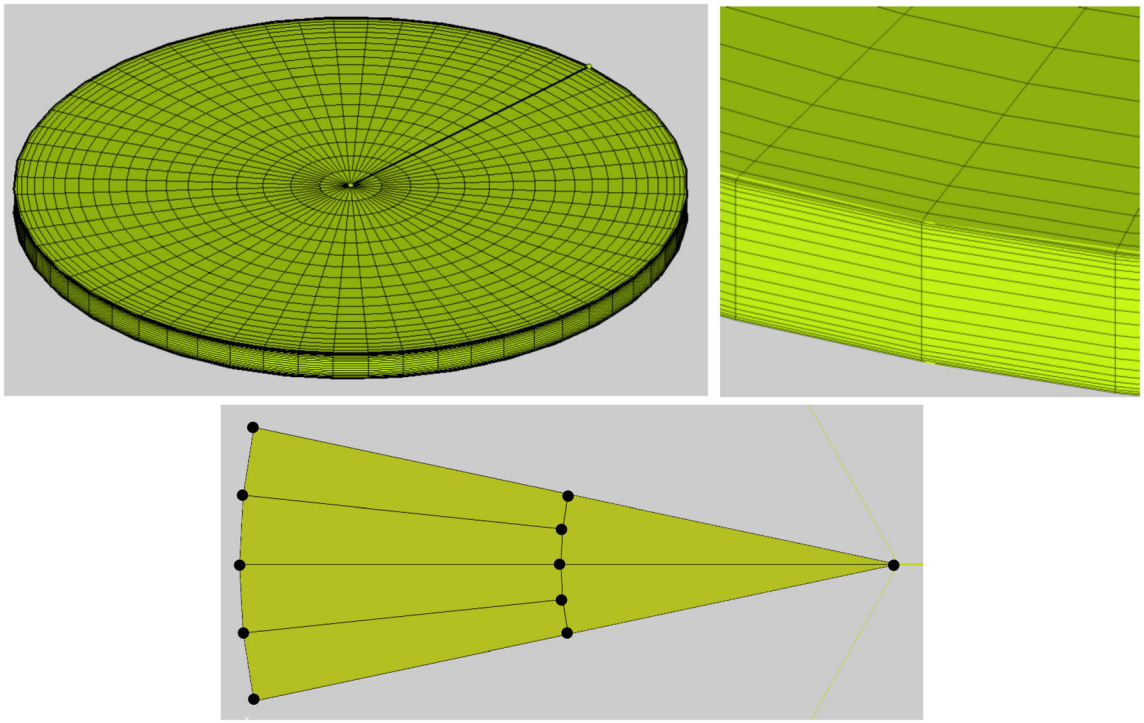

FIGURE 9 Mesh used for disk samples, finer near exposed surfaces [Color figure can be viewed at wileyonlinelibrary.com]

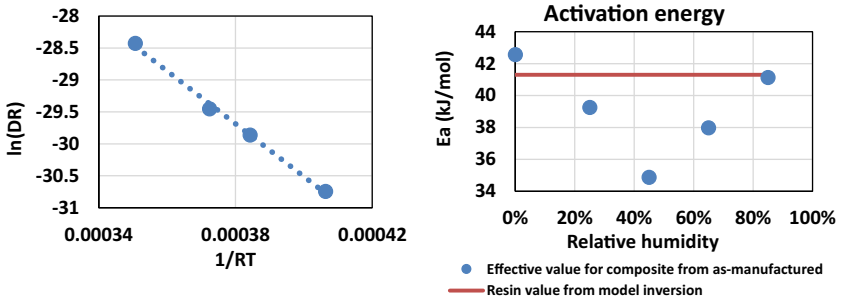

FIGURE 10 (A) Arrhenius plot for derived resin directional diffusion coefficient; (B) comparison of resin activation energy and composite effective activation energy [Color figure can be viewed at wileyonlinelibrary.com]

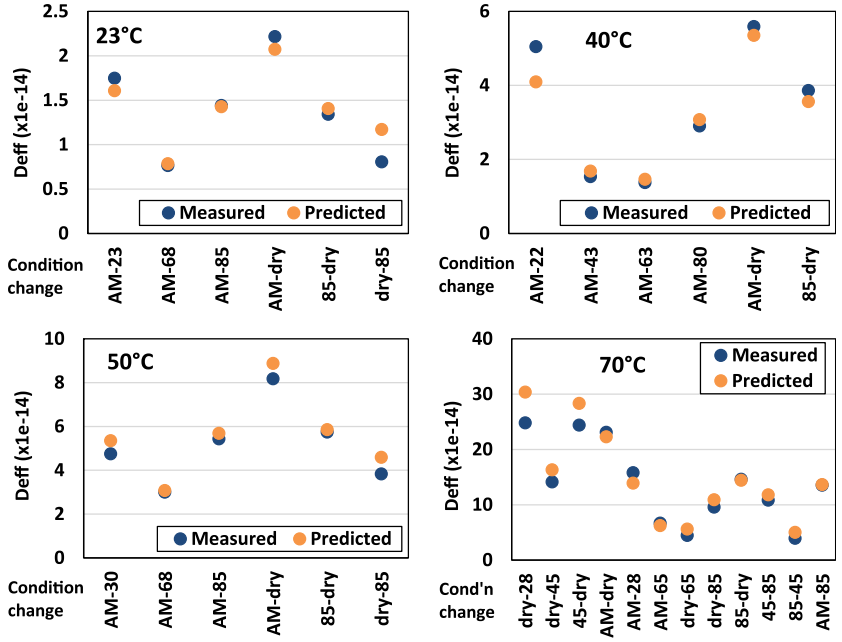

FIGURE 11 Comparison of predicted and measured effective diffusion coefficients for composite samples [Color figure can be viewed at wileyonlinelibrary.com]

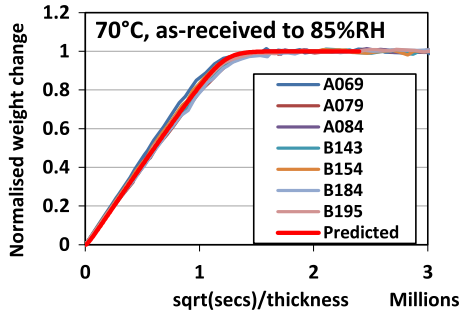

FIGURE 12 Example of well-predicted water uptake curve (separate experimental samples are shown with individual sample number) [Color figure can be viewed at wileyonlinelibrary.com]

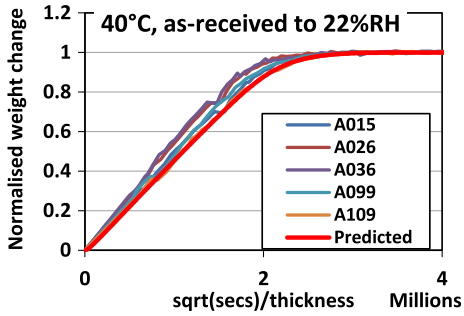

FIGURE 13 Example of least well-predicted water uptake curve for samples from as-manufactured state [Color figure can be viewed at wileyonlinelibrary.com]

relative humidity, which would not normally have any reasonable explanation. However, while the overall activation energy for the composite would mainly result from that for the resin diffusion coefficient, it also has components from the fiber adsorption and pore absorption (Equation 17). Depending on the activity change taking place, these components have different relative impacts, so, for example, for samples staying mostly in the mid-activity range pore absorption has a significant effect. When these are taken account of, the activation energy for the remaining resin diffusion coefficient was found to have a sensible value.

8 | RESULTS

The difference between predicted and measured effective diffusion coefficients is shown in Figure 11. For the condition change labels, as-manufactured is indicated as AM, and the figures are the actual RHs (%) at each temperature. In the majority of cases, a good match was achieved; however, there were some outliers. Selected corresponding water uptake curves are shown in

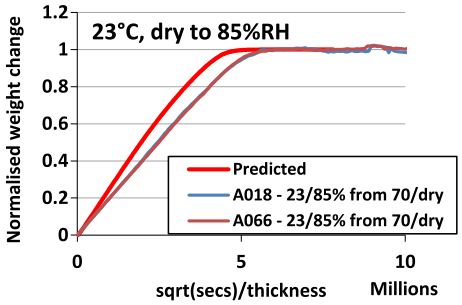

FIGURE 14 Poorly predicted water uptake curve corresponding to outlier in Figure 11 [Color figure can be viewed at wileyonlinelibrary.com]

Figures 12–14. Because there was some variability in the samples used and the measured data, the curves have been normalized for comparison. The x-axis shows (√secs)/thickness, and the y-axis is scaled so that all samples change from 0 to 1.

Although there were only a few poor predictions, these could not be explained by minor changes to the model as formulated. This suggests an additional behavior that is not being taken account of. One possibility is a resistance to water movement either in or out of the fibers, and this is a potential area for extension of the model. Diffusion along the surface of the fibers, and the interaction of that with the adsorbed water, is also a possibility.

The water absorption curves and diffusion coefficients obtained corresponded to the specific fiber/matrix interface and interphase of the material used. A different fiber surface treatment might be expected to change these, and correspondingly the parameters derived for the model. Changes to the interface and fiber surface energy could affect the rate and quantity of adsorption of water molecules on to the fiber surface, and the energy required for clusters of molecules to move between the fiber surface and the fiber pores. These would change the adsorption and absorption curves shown in Figure 6. In addition, any effect on the interphase region could change the overall resin diffusion coefficient. These effects would not change the principles behind the model described here, but further extension could look at explicitly taking account of the effect of fiber surface treatment on the model parameters.

9 | CONCLUSIONS

The water absorption and diffusion behavior were characterized for a composite comprising activated carbon fibers in a resole phenolic resin. The behavior observed

was quite complex, due to a combination of water adsorbed on to and absorbed into the fibers and the water in the resin from curing. This gave very nonlinear absorption with humidity, together with measured "effective" diffusion coefficients that varied strongly with starting and end conditions.

This is significant in practical applications for a number of reasons. If a specific uniform water content is required, either for use or material testing, the time needed to achieve this may vary by factors of two or three. If this time is underestimated, then the water content will be nonuniform leading to variable properties through the material. In applications where polymer degradation is related to water content, the timescale of degradation in the presence of a porous substrate may be very different from that for the polymer alone.

A "source-sink" model has been successfully developed to simulate this absorption and diffusion behavior. Water was assumed to diffuse only through the phenolic resin, in a simple Fickian manner, but water molecules were adsorbed on to the fiber surfaces then when sufficient were present migrated in clusters into the fiber pores. The fibers therefore acted as a source or sink of water, and while water was moving between resin and fibers diffusion through the resin was slowed down. This process was successfully simulated by an extended Fickian model which took account of the nonlinear water uptake behavior of the fibers. In most cases, the model could replicate closely the weight change behavior of test samples moved between different humidity conditions at a range of temperatures. There were, however, a few examples where the measured data were less closely followed, suggesting that other processes may be affecting the behavior, which have yet to be included. The most likely reason for this is some small activation energy barriers to water moving into or out of the pores in the fibers, which was not included in the model, but may be required for any future development. Further extension of the model could explicitly include the effect of surface treatment on water movement in and out of the fibers, and take account of different diffusion through the interphase region.

The demanding applications in which this material is used make it particularly important to be able to predict its water content in order to ensure the required performance is achieved. The porosity of the fibers means that this cannot be achieved using a conventional Fickian model, but a high degree of accuracy can be obtained using the proposed "source-sink" extended model.

ACKNOWLEDGMENTS

This work was supported by the Defence Science and Technology Laboratory, UK.

NOMENCLATURE

a	activity (dimensionless)
a_{lim}	activity above which no more adsorption takes place (dimensionless)
c_R	mass concentration of water in resin (kg/m^3)
c_F	mass concentration of water in fibers (kg/m^3)
c	mass concentration of water in the composite (kg/m^3)
D	effective diffusion coefficient through composite (m^2/s)
D_R	average diffusion coefficient through the resin when in the composite (m^2/s)
D_{Resin}	diffusion coefficient through the resin alone (m^2/s)
D_0	temperature-independent pre-exponential for Arrhenius equation (m^2/s)
E_a	activation energy for Arrhenius equation (J/mol)
F	resin transport ratio, that is, fraction of water movement which is through the resin rather than migration into or out of the fibers (dimensionless)
h	sample thickness (m)
$\underline{J}$	mass flux (kg/(m^2.s)
k	factor representing the microstructure (dimensionless)
M_t	weight change at time t (dimensionless)
M_∞	total weight change when a steady state is reached (dimensionless)
R	gas constant (J/mol-K)
s_R	resin saturation water content (kg/m^3), that is, value at 100% activity
s_a	saturation for adsorbed water content (kg/m^3), that is, value at 100% activity
s_p	saturation for pore water content (kg/m^3), that is, value at 100% activity
t	conditioning time (s)
T	sample temperature (K)
V_f	fiber volume fraction (dimensionless)

ORCID

Sue Alston https://orcid.org/0000-0003-0496-3296
Cris Arnold https://orcid.org/0000-0002-8937-1355

REFERENCES

[1] J. Feldman, D. Ellerby, M. Stackpoole, K. Peterson, E. Venkatapathy, NASA website. https://ntrs.nasa.gov/archive/nasa/casi.ntrs.nasa.gov/20150022378.pdf. .
[2] E. H. Stokes, *AIAA J.* **1992**, *30*, 1597.
[3] P. Bonniau, A. R. Bunsell, *J. Compos. Mater.* **1981**, *15*, 272.
[4] F. Korkees, S. Alston, C. Arnold, *Polym. Compos.* **2017**, *39*, E2305.

[5] S. Alston, F. Korkees, C. Arnold, Proceedings of ECCM15 – 15th European Conference on Composite Materials, June 24–28, 2012, Venice, Italy. Paper 2303. http://www.escm.eu.org/eccm15/data/assets/2303.pdf (accessed: January 2020).
[6] H. G. Carter, K. G. Kibler, *J. Compos. Mater.* **1978**, *12*, 118.
[7] L. A. Rodriguez, A. Damley-Strnad, L. R. Grace, *J. Reinf. Plast. Comp.* **2019**, *38*, 628.
[8] L. R. Grace, M. C. Altan, *Polym. Compos.* **2013**, *34*, 1144.
[9] S. Popineau, C. Rondeau-Mouro, C. Sulpice-Gaillet, M. E. R. Shanahan, *Polymer* **2005**, *46*, 10733.
[10] Q. Liu, D. De Kee, R. K. Gupta, *AIChE J.* **2008**, *54*, 364.
[11] Y. Joliff, L. Belec, M. B. Heman, J. F. Chailan, *Comput. Mater. Sci.* **2012**, *64*, 141.
[12] H. Liang, H. Xing, M. Qin, H. Wu, *Compos. Part A* **2020**, *135*, 105959. https://doi.org/10.1016/j.compositesa.2020.105959.
[13] G. Li, T. Xie, S. Yang, J. Jin, J. Jiang, *J. Phys. Chem. C* **2012**, *116*, 9196.
[14] A. D. Roberts, J.-S. M. Lee, A. Magaz, M. W. Smith, M. Dennis, N. S. Scrutton, J. J. Blaker, *Molecules* **2020**, *25*, 1207.
[15] D. D. Do, H. D. Do, *Carbon* **2000**, *38*, 767.
[16] I. Rajzer, E. Menaszek, L. Bacakova, M. Rom, M. Blazewicz, *J. Mater. Sci.: Mater. Med.* **2010**, *21*, 2611.
[17] A. Gusain, R. M. Faria, P. B. Miranda, *Front. Chem* **2019**, *7*, 61.
[18] S. Schusser, A. Poghossian, M. Bäcker, M. Leinhos, P. Wagner, M. J. Schöning, *Sens. Actuators B* **2013**, *187*, 2. https://doi.org/10.1016/j.snb.2012.07.099.
[19] P. Yang, Q. Zhou, X.-X. Yuan, J. M. N. van Kasteren, Y.-Z. Wang, *Polym. Degrad. Stabil.* **2012**, *97*, 1101. https://doi.org/10.1016/j.polymdegradstab.2012.04.007.
[20] I. M. Smith, D. V. Griffiths, *Programming the Finite Element Method*, 3rd ed., John Wiley & Sons, Chichester **1998**.
[21] Z. Huo, V. Bheemreddy, K. Chandrashekhara, R. A. Brack, *J. Compos. Mater.* **2015**, *49*, 321.

How to cite this article: Alston S, Arnold C, Swan M, Stone C. A source-sink model for water diffusion in an activated carbon fiber/phenolic composite. *Polymer Composites*. 2021;1–12. https://doi.org/10.1002/pc.26078